

Fig. 1 Conic trajectory and velocity components

From the triangle of velocities  $\triangle BCD$ , one has the equation of special hodograph:

$$(V_\theta - V_h)^2 + V_r^2 = V_p^2$$

In the plane  $V_\theta, V_r$ , this hodograph is a circle; its center is placed on  $V_\theta$  axis at a distance  $V_h$  from the origin, and its radius is equal to  $V_p$  (Fig. 3).

It is clear that both the classical and special polar hodographs are valid for all classes of conic figures, i.e., elliptic, parabolic, and hyperbolic. Different classes of conic figures are provided by attendant changes of  $V_p$  and  $V_h$ .

For elliptical orbit,

$$e < 1 \quad V_p < V_h$$

for parabolic orbit,

$$e = 1 \quad V_p = V_h$$

and for hyperbolic orbit,

$$e > 1 \quad V_p > V_h$$

### Conclusions

The orbital velocity in the two-body orbital motion can be resolved into two components of invariant magnitude:  $V_h$ , normal to the radius vector, and  $V_p$ , normal to the line of apsides. These components are important for both the classical and special hodograph. In the classical hodograph,  $V_h$  is the radius of the hodograph and  $V_p$  is the ordinate of its center. In the special hodograph,  $V_p$  is the radius of the hodograph and  $V_h$  is the abscissa of its center.

### References

- 1 Cronin, J. L. and Schwartz, R. E., "Invariant two-body velocity components," *J. Aerospace Sci.* **29**, 1384-1385 (1962).
- 2 Altman, S. P. and Pistiner, J. S., "Hodograph transformations and mapping of the orbital conics," *ARS J.* **32**, 1109-1111 (1962).
- 3 Fang-Toh-Sun, "Some applications of the special hodograph for orbital motion," *Proceedings of the Third International Symposium on Rockets and Astronautics, Tokyo, 1962* (Yokendo, Bunkyo-Ku, Tokyo, 1962), pp. 381-396.
- 4 Altman, S. P. and Pistiner, J. S., "Polar hodograph for ballistic missile trajectories," *ARS J.* **31**, 1592-1594 (1961).

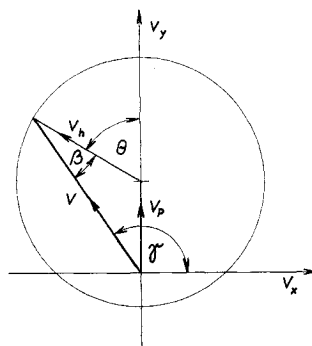
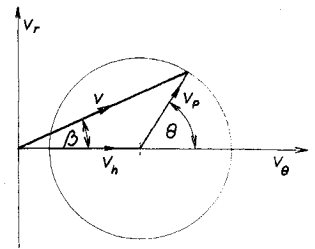


Fig. 2 Classical hodograph

Fig. 3 Special hodograph



<sup>5</sup> Altman, S. P. and Pistiner, J. S., "Hodograph analysis of the orbital transfer problem for coplanar nonaligned elliptical orbits," *ARS J.* **31**, 1217-1235 (1961).

<sup>6</sup> Fang-Toh-Sun, "A special hodograph for orbital motion," *Proceedings of the Second International Symposium on Rockets and Astronautics, Tokyo, 1960* (Yokendo, Bunkyo-Ku, Tokyo, 1961), pp. 163-189.

## Integration of the Velocity Equation of the Laminar Boundary Layer Including the Effects of Mass Transfer

H. L. EVANS\*

Imperial College, London, England

A METHOD is given for obtaining numerical solutions to the differential equation that governs fluid motion in a similar, laminar boundary layer. When some of the fluid flows in either direction through the wall, the problem contains two parameters, one being associated with the pressure gradient in the freestream while the other is a measure of the rate of mass transfer through the wall. The method of integration is quite general and gives high accuracy for any values of these parameters; it is particularly useful under conditions when other methods break down.

Spalding<sup>1</sup> has shown that the velocity equation of the uniform property, laminar boundary layer possesses similar solutions when the freestream velocity  $u_G$  obeys the relation

$$(du_G/dx) = C u_G^{2(\beta-1)/\beta} \quad (1)$$

where  $C$  and  $\beta$  are constants, the latter being the parameter associated with the freestream pressure gradient, and the  $x$  direction is parallel to the wall. When  $\eta$  the dimensionless distance from the wall, and  $f$  the dimensionless stream function are defined as

$$\eta = y \left( \frac{1}{\beta \nu} \frac{du_G}{dx} \right)^{1/2} \quad (2)$$

$$f = \frac{\psi}{u_G} \left( \frac{1}{\beta \nu} \frac{du_G}{dx} \right)^{1/2} \quad (3)$$

where  $y$  is the distance perpendicular to the wall,  $\nu$  is the kinematic viscosity, and  $\psi$  the ordinary stream function, the differential equation for similar boundary layers takes the form

$$f''' + ff'' + \beta(1 - f'^2) = 0 \quad (4)$$

with the boundary conditions

$$\begin{aligned} \eta = 0 \quad f = f_0 \quad f' = 0 \\ \eta \rightarrow \infty \quad f' \rightarrow 1 \end{aligned} \quad (5)$$

The primes in Eqs. (4) and (5) denote differentiation with

Received March 25, 1963.

\* Lecturer, Department of Mechanical Engineering.

respect to the independent variable  $\eta$ , and the quantity  $f_0$ , which is a constant for similar boundary layers, is related to the rate of mass transfer through the wall and may be positive or negative depending on the direction of mass transfer.

In order to integrate Eq. (4) for specific values of the parameters  $\beta$  and  $f_0$ , the corresponding dimensionless wall shear  $f_0''$  must be known accurately. When  $f_0$  is small in magnitude,  $f_0''$  must be obtained by trial and error, although many values already are known for wide ranges in  $\beta$ . For intensive inward mass transfer, it approaches the following asymptote that is simply the series given by Watson<sup>2</sup> extended by one term:

$$\frac{f_0''}{f_0} = 1 + \frac{a_1}{f_0^2} + \frac{a_2}{f_0^4} + \frac{a_3}{f_0^6} + \frac{a_4}{f_0^8} + \frac{a_5}{f_0^{10}} + \dots \quad (6)$$

where the coefficients are

$$\begin{aligned} a_1 &= (1 + 3\beta)/2 \\ a_2 &= -(5 + 18\beta + 16\beta^2)/6 \\ a_3 &= (550 + 2303\beta + 3098\beta^2 + 1417\beta^3)/144 \\ a_4 &= -(117,096 + 552,179\beta + 932,317\beta^2 + 694,741\beta^3 + \\ &\quad 200,207\beta^4)/4320 \\ a_5 &= (131,557,872 + 681,840,181\beta + 1,345,537,521\beta^2 + \\ &\quad 1,302,524,188\beta^3 + 635,230,092\beta^4 + \\ &\quad 128,414,716\beta^5)/518,400 \end{aligned}$$

Equation (6) gives high accuracy when  $f_0$  is greater than 3.0.

The corresponding asymptote for intensive outward mass transfer is

$$-\frac{f_0''}{f_0} = \frac{b_1}{f_0^2} + \frac{b_2}{f_0^6} + \frac{b_3}{f_0^{10}} + \frac{b_4}{f_0^{14}} + \dots \quad (7)$$

in which the coefficients are

$$\begin{aligned} b_1 &= \beta \\ b_2 &= (1 - 2\beta)\beta^2 \\ b_3 &= (13 - 18\beta)(1 - 2\beta)\beta^3 \\ b_4 &= (448 - 1098\beta + 684\beta^2)(1 - 2\beta)\beta^4 \\ b_5 &= (29,075 - 96,262\beta + 107,948\beta^2 - 41,048\beta^3) \times \\ &\quad (1 - 2\beta)\beta^5 \\ b_6 &= (3,052,533 - 12,307,766\beta + 18,883,332\beta^2 - \\ &\quad 13,082,408\beta^3 + 3,456,288\beta^4) \cdot (1 - 2\beta)\beta^6 \\ b_7 &= (473,813,584 - 2,207,664,996\beta + 4,168,446,244\beta^2 - \\ &\quad 3,991,748,504\beta^3 + 1,940,450,160\beta^4 - \\ &\quad 383,354,208\beta^5) \cdot (1 - 2\beta)\beta^7 \end{aligned}$$

Equation (7) gives high accuracy when  $f_0$ , whose sign is now negative, satisfies  $|f_0| \geq 2.0$ . Near  $f_0 = -2.0$  its accuracy is improved by application of the Euler transformation. A detailed discussion of the derivation of Eqs. (6) and (7) is to be published elsewhere.

When Eq. (4) is integrated by the usual numerical methods starting at  $\eta = 0$ , the freestream boundary condition that  $f' \rightarrow 1$  as  $\eta \rightarrow \infty$  is difficult to satisfy accurately for many values of  $\beta$  and  $f_0$ . Eckert, Donoughe, and Moore,<sup>3</sup> for example, found that as the amount of fluid moving out from the wall increased, the wall shear  $f_0''$  had to be specified more and more accurately; for  $\beta = 1.0$ , when  $f_0$  reached  $-3.0$ , the freestream boundary condition could not be satisfied to four digits even when  $f_0''$  was known to 10 digits. The

same difficulty arises in the imaginary domain relating to Eq. (4) (see Spalding and Evans<sup>4</sup>) even when no fluid flows through the wall, because the forward velocity of the fluid then approaches its freestream value very gradually. These difficulties, to a large extent, are overcome by the method of integration proposed below.

The order of Eq. (4) is reduced first by taking the fluid velocity  $f'$  as the independent variable and the velocity gradient  $f''$  as the dependent variable; for the sake of clarity, the symbols

$$f' = \varphi \quad f'' = \gamma \quad (8)$$

are employed. When the relationships

$$f''' = \gamma \frac{d\gamma}{d\varphi} \quad f = f_0 + \int_0^\eta f' d\eta \quad d\eta = \frac{d\varphi}{\gamma}$$

are applied to Eq. (4) and the resulting equation is divided by  $\gamma$ , there results

$$\frac{d\gamma}{d\varphi} + f_0 + \int_0^\varphi \frac{\varphi}{\gamma} d\varphi + \beta \frac{(1 - \varphi^2)}{\gamma} = 0 \quad (9)$$

The ranges of the variables in this equation are  $0 \leq \varphi \leq 1.0$  and  $f_0'' \leq \gamma \leq 0$ , although there are some exceptions to the latter when, as happens near separation, the shear stress is lower at the wall than in the boundary layer. In these new coordinates, the displacement and momentum thicknesses are

$$\delta_1^* = \int_0^1 \frac{(1 - \varphi)}{\gamma} d\varphi \quad \delta_2^* = \int_0^1 \frac{\varphi(1 - \varphi)}{\gamma} d\varphi$$

The second and third terms in Eq. (9) together represent the dimensionless stream function  $f$ , which becomes infinite at  $\varphi = 1$  where  $\gamma = 0$ . The equation therefore possesses a singularity at  $\varphi = 1$ , but this causes only minor difficulties when integration proceeds from  $\varphi = 0$  towards  $\varphi = 1$ .

It should be realized that when  $f_0''$  is known for specified values of  $\beta$  and  $f_0$ , if the quantity  $(\delta_1^* - \delta_2^*)$  can be evaluated accurately by numerical methods, both the displacement and the momentum thickness can then be obtained from the exact relationship,

$$f_0'' = f_0 + \beta\delta_1^* + (\beta + 1)\delta_2^* \quad (10)$$

Other functions of the velocity layer can then be calculated from known formulas (Spalding and Evans<sup>4</sup>). The remainder of the note will consider how to evaluate  $(\delta_1^* - \delta_2^*)$ .

The following definitions are introduced:

$$g = \int_0^\varphi \frac{\varphi}{\gamma} d\varphi \quad h = \int_0^\varphi \frac{(1 - \varphi)^2}{\gamma} d\varphi$$

where both  $g$  and  $h$  are functions of the independent variable  $\varphi$  and the value of  $h$  at  $\varphi = 1$  is the required quantity  $(\delta_1^* - \delta_2^*)$ .

In order to evaluate this, the following set of differential equations must be integrated numerically using, for example, a Runge-Kutta process:

$$d\gamma/d\varphi = -\{f_0 + g + \beta[(1 - \varphi^2)/\gamma]\} \quad (11)$$

$$dg/d\varphi = \varphi/\gamma \quad (12)$$

$$dh/d\varphi = (1 - \varphi)^2/\gamma \quad (13)$$

Starting values for the functions and their gradients are obtained simply by inserting the values  $\varphi = 0$  and  $\gamma = f_0''$  into the appropriate equation or definition.

Most solutions to Eq. (9) behave like that for  $\beta = 1.0$  and  $f_0 = -2.0$  shown in Fig. 1. This solution corresponds to a moderate rate of fluid flow directed outward from the wall. The asymmetry of  $\varphi(1 - \varphi)/\gamma$ , the integrand in the momentum thickness  $\delta_2^*$ , is a characteristic feature of solutions with or without fluid flowing through the wall. The figure shows the variation with  $\varphi$  of  $4\gamma$  and the integrands

of  $\delta_1^*$ ,  $\delta_2^*$ , and  $h$ ; the vertical scale for  $\gamma$  was magnified four times in order to show the curvature better.

Close to  $\varphi = 1$  the contribution to  $h$ , represented by the area under the curve of  $(1 - \varphi)^2/\gamma$ , is appreciably less than the contribution to either  $\delta_1^*$  or  $\delta_2^*$ . The gradient of the integrand in  $h$  is also much smaller in that region than the gradients of the integrands in  $\delta_1^*$  and  $\delta_2^*$ .

When Eqs. (11-13) are integrated numerically, an interval of  $\Delta\varphi = 0.01$  generally gives high accuracy, although some solutions would need a slightly smaller value. The dependent variable  $\gamma$  behaves well and can be obtained accurately up to  $\varphi = 0.99$ , but soon after that high accuracy is difficult to achieve because  $d\gamma/d\varphi$  in Eq. (12) is then very large. No matter how accurate  $f_0''$  may be, because of the singularity mentioned earlier, it is always difficult to make  $\gamma$  very small at  $\varphi = 1$  where it should, in fact, be zero. Fortunately, however, the effect on  $h$  is negligible and the method gives  $h(1) = (\delta_1^* - \delta_2^*)$  at least as accurately as the most accurate solutions found in the literature.

Most methods of integrating Eq. (4) give high accuracy when the velocity  $f'$  (or  $\varphi$ ) is in the range  $0 \leq f' \leq 0.99$ , but

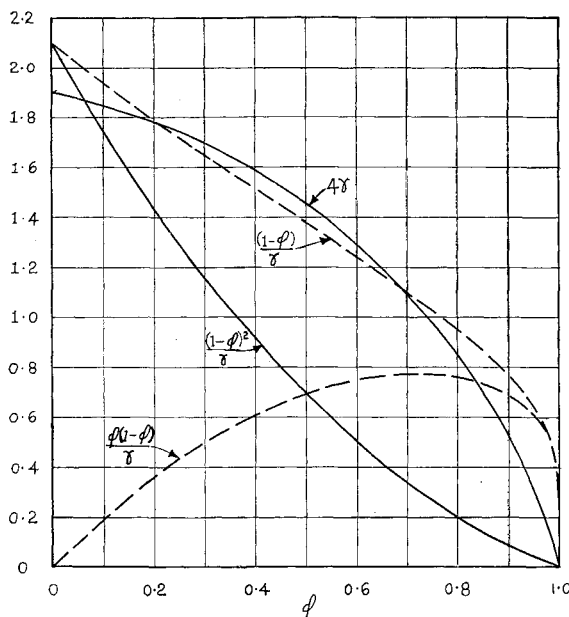


Fig. 1 Variation of  $4\gamma$  and the integrands in  $\delta_1^*$ ,  $\delta_2^*$ , and  $h$  with the fluid velocity  $\varphi$  for the typical solution  $\beta = 1.0$ ,  $f_0 = -2.0$

some tend to break down between  $f' = 0.99$  and  $f' = 1.0$ . The present method has the advantage that integration over this last interval can often be achieved in one step, and more than three steps would rarely be necessary.

The following method of completing the integration is also found to work well. The contribution to  $(\delta_1^* - \delta_2^*)$  up to  $\varphi = 0.98$  is given accurately by the integration process just described, as also are the values of  $\gamma$  at  $\varphi = 0.98$  and  $\varphi = 0.99$ . Since the integrand in  $h$  is necessarily zero at  $\varphi = 1.0$ , the small contribution from the range  $0.98 \leq \varphi \leq 1.0$  is evaluated readily by Simpson's rule.

As an example, the method was applied to the two-dimensional forward stagnation point with no fluid flowing through the wall. With the following data  $\beta = 1.0$ ,  $f_0 = 0$ ,  $f_0'' = 1.2325877$ , and  $\Delta\varphi = 0.01$ , the method gave  $(\delta_1^* - \delta_2^*) = 0.3555568$ . In order to obtain a solution of comparable accuracy by integrating Eq. (4) directly, the wall shear  $f_0''$  was obtained to three more digits by trial and error. With  $f_0'' = 1.232587604$  and an interval of  $\Delta\gamma = 10/128$  this method gave  $(\delta_1^* - \delta_2^*) = 0.3555572$ , where there is uncertainty about the last digit. The difference between the two values is clearly negligible.

## References

- <sup>1</sup> Spalding, D. B., "Mass transfer through laminar boundary layers, 1: The velocity boundary layer," *Intern. J. Heat Mass Transfer* 2, 15-32 (1961).
- <sup>2</sup> Watson, E. J., "Asymptotic theory of boundary layer flow with suction," *Brit. Aeronaut. Res. Council, Res. and Memo.* 2619 (1952).
- <sup>3</sup> Eckert, E. R. G., Donoughe, P. L., and Moore, B. J., "Velocity and friction characteristics of laminar viscous boundary-layer and channel flow over surfaces with ejection or suction," *NACA TN 4102* (1957).
- <sup>4</sup> Spalding, D. B. and Evans, H. L., "Mass transfer through laminar boundary layers, 2: Auxiliary functions for the velocity boundary layer," *Intern. J. Heat Mass Transfer* 2, 199-221 (1961).

## Impulse Bit Measurement for Small Pulsed Rocket Motors

P. S. STARRETT\* AND P. F. HALFPENNY†

Lockheed California Company, Burbank, Calif.

Conservation of propellants in attitude control for spacecraft often requires delivery of a low thrust in very short pulses. A method for measurement of the integrated impulse bit using a swinging pendulum is described. Some of the results in the successful application of this technique to an experimental program on cold gas propellants are presented.

**D**URING a research program on the performance attainable with selected cold gas propellants in an attitude control system, it was necessary to devise a method of determining the effective specific impulse for very short pulses. The work done covered pulse durations from 25 to 125 msec and thrusts of 1 to 10 lb, although the method is certainly adaptable to shorter pulses and smaller thrusts.

Load cell measurements of short pulses tend to become cluttered with extraneous oscillations of the system under test, making the data difficult to reduce. Also, inertial forces induced by closing and opening the valve solenoids produce confusing indications. Therefore, measurement of the integrated effect of the impulse bit appeared to be a desirable goal. Several methods of accomplishing this were examined. A technique finally was selected which involved measuring the impulse received by a swinging pendulum. The advantages of this approach were 1) all dynamic events occurring during the pulse were integrated and the net effect observed; 2) the measurement was essentially a primary one, depending only on a proper measurement and interpretation of the pendulum dynamics; and 3) the design and fabrication costs would be very modest.

## Swinging Pendulum Technique

In the study of cold gas propellants, all components were supported on the pendulum, as shown in Fig. 1, and the pendulum was suspended by a crossed-pivot flexure from a rigid attachment. A knife edge support also was tried but resulted in higher decay rates. Instrumentation and control lines from the pressure and temperature transducers and the valve pulse circuit were brought through the plane of the flexure to minimize their effect on the pendulum performance.

The impulse imparted to the pendulum by a pulse could be evaluated either in terms of a change in pendulum ampli-

Received April 1, 1963.

\* Group Engineer, Thermodynamic Systems Research. Member AIAA.

† Research Specialist, Thermodynamic Systems Research.